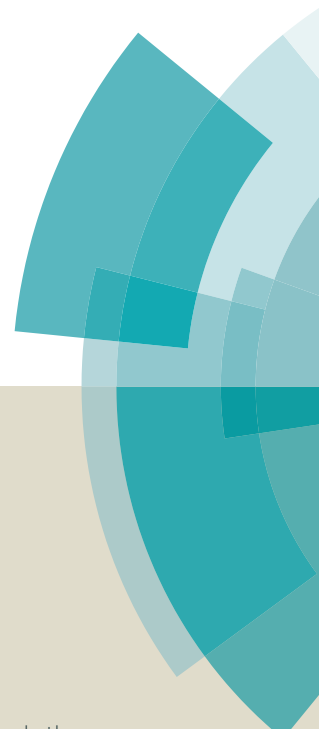
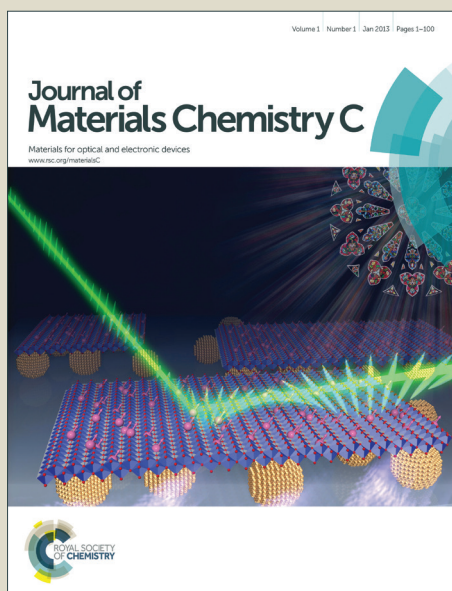


Journal of Materials Chemistry C

Accepted Manuscript



This article can be cited before page numbers have been issued, to do this please use: R. Wei, Z. Xu, X. Liu, Y. He and X. G. Wang, *J. Mater. Chem. C*, 2015, DOI: 10.1039/C5TC02126J.



This is an *Accepted Manuscript*, which has been through the Royal Society of Chemistry peer review process and has been accepted for publication.

Accepted Manuscripts are published online shortly after acceptance, before technical editing, formatting and proof reading. Using this free service, authors can make their results available to the community, in citable form, before we publish the edited article. We will replace this *Accepted Manuscript* with the edited and formatted *Advance Article* as soon as it is available.

You can find more information about *Accepted Manuscripts* in the [Information for Authors](#).

Please note that technical editing may introduce minor changes to the text and/or graphics, which may alter content. The journal's standard [Terms & Conditions](#) and the [Ethical guidelines](#) still apply. In no event shall the Royal Society of Chemistry be held responsible for any errors or omissions in this *Accepted Manuscript* or any consequences arising from the use of any information it contains.

ARTICLE

Liquid-crystalline compounds containing both strong *push-pull* azo chromophore and cholesteryl unit as photoresponsive molecular glass materials

Cite this: DOI: 10.1039/x0xx00000x

Renbo Wei,^{a,b} Zeda Xu,^c Xiyang Liu,^a Yaning He,^a and Xiaogong Wang^{a*}Received 00th January 2015,
Accepted 00th January 2015

DOI: 10.1039/x0xx00000x

www.rsc.org/

A series of liquid-crystalline (LC) compounds (R-Chol, R: CA, CN and NT), containing both a strong *push-pull* azo chromophore and a cholesteryl unit, was synthesized as novel molecular glass materials. The molecular structures and phases of the condensed state were characterized by spectral analyses, DSC, XRD and POM. The azo compounds existed as glassy solid at room temperature and entered smectic LC phase above glass transition temperature. Optical-quality solid films of R-Chol were obtained by spin-coating. The spin-coated films of CA-Chol and CN-Chol existed in the amorphous state and only NT-Chol film showed weak birefringence and polydomain texture. Upon irradiation with a linearly polarized Ar⁺ laser (488 nm) beam, photoinduced orientation rapidly developed for CA-Chol and CN-Chol films, which showed significant photoinduced birefringence and dichroism. When the irradiating light was switched off, the birefringence did not show decay relaxation as a usual case, but showed a small increase in the relaxation process. Photoinduced surface-relief-grating (SRG) formation was investigated by irradiating the films with two *p*-polarized interfering Ar⁺ laser beams. SRGs formed on the CA-Chol films showed the highest inscription rate in the series. The efficiencies of both photoinduced orientation and SRG formation were enhanced for the azo chromophore bearing the carboxylic group as the electron-withdrawing substituent. Two-dimensional (2D) quasi-crystal structures with 10- and 12-fold rotation symmetries were successfully fabricated on the CN-Chol films by using the dual-beam multiple exposure technique. The capability of the materials as a photo-storage medium was demonstrated by holographic recording.

Introduction

Azobenzene and its derivatives have been widely used as functional building blocks to construct polymeric materials with various photoresponsive properties.^[1-10] Upon irradiation with light at appropriate wavelengths, azo polymers can show a variety of photoresponsive properties related to the reversible *trans-cis* isomerization of azo chromophores.^[1,2,11] The repeated photo-isomerization of the azo chromophores can trigger motions at different levels.^[5] At the molecular level, repeated cycles of *trans-cis-trans* isomerization drive the azo chromophores in the polymers to take preferential orientation in a direction perpendicular to the light polarization plane.^[12] The orientation can also cause some correlative alignments of groups and segments adjacent to the azo chromophores. The irradiation-driven orientation results in the photoinduced anisotropy (PIA) of solid thin films to show optical dichroism and birefringence.^[2,4,5] At the micrometer level, the photo-isomerization induces mass transport of azo polymers. Upon irradiation with interfering laser beams, surface-relief-gratings (SRGs) can be inscribed on the azo polymer films.^[13,14] SRGs are formed at a temperature well below the glass transition

temperature (T_g) of the polymers and can be erased by heating sample to a temperature above its T_g .^[3,5] Driven by photoisomerization, azo polymers can show other interesting photoresponsive functions, such as photoinduced phase transition,^[15] spontaneous surface pattern formation,^[16] photo-mechanical thin film contraction and bending,^[17-19] and photoinduced colloidal deformation.^[20]

Distinct from the azo polymers, amorphous molecular materials (also named molecular glass) have recently been developed as a medium to contain azo chromophores for optical and photonic applications.^[21-25] The glassy materials consist of some well-designed low-molecular-weight organic compounds to show glass-transition behavior similar to amorphous polymers.^[22-24] Amorphous molecular materials possess well-defined structures and often show better reproducible properties compared with polymers. By using the common spin-coating method, thin solid films with a smooth surface can be feasibly prepared by using the amorphous molecular materials. Films of azo molecular glasses have been used for inscribing SRGs and other surface patterns.^[22,24,25] Results show that SRGs can be inscribed on azo molecular glass films with a faster rate compared to those usually observed for azo polymers. Because of the well-defined structures, amorphous molecular materials

could be a desirable type of materials to study the structure-property relationship and for future device applications as well.

Typical amorphous molecular materials are designed to possess rigid molecular structures to contain one or two azobenzene moieties, which can readily form stable amorphous glasses at high temperature.^[22-24] Recently, three-arm or star-shape molecular glasses have been developed for inscribing SRG and other optical applications.^[26-30] Flexible linkages have been introduced into the molecular structures and some of the compounds show liquid crystallinity too. In addition to the branched molecules, a series of linear molecules linking an azo chromophore to a rigid biphenylene unit through a flexible spacer have also been synthesized.^[31,32] Upon Ar⁺ laser irradiation, photoinduced orientation can be rapidly induced for the molecular glasses to show significant birefringence and dichroism. SRG can also be efficiently inscribed on the film surfaces. According to the spectral feature and isomerization behavior, azo chromophores have been classified into azobenzene type, aminoazobenzene type, and pseudo-stilbene type.^[11] The pseudo-stilbene (*push-pull*) type azo chromophores contain strong electron-donating/-withdrawing substituents at 4 and 4' positions of the azobenzene moieties. These *push-pull* type azo chromophores possess strong absorption bands in visible light region due to $\pi \rightarrow \pi^*$ electronic transition. Polymers containing such chromophores can show a variety of photoresponsive functions caused by the fast *trans-to-cis* isomerization and thermal relaxation.^[2,5] It is of particular interest to develop amorphous molecular materials with simple structures to contain the *push-pull* type azo chromophores in a high density. To our knowledge, there are only few reports available for this type of the molecular glasses.

In this study, a series of compounds containing both a strong *push-pull* azo chromophore and a cholesteryl group was synthesized. The molecules were constructed by connecting the azo chromophore and cholesteryl unit via a flexible spacer (**Figure 1**). The materials showed liquid crystallinity above T_g , as indicated by differential scanning calorimetry (DSC), X-ray diffraction (XRD) and polarized optical microscopy (POM). On the other hand, high transparent solid films could be obtained by spin-coating of the azo compound solutions. The properties of the azo molecular glasses, especially those related with their responses to light irradiation, were investigated in detail.

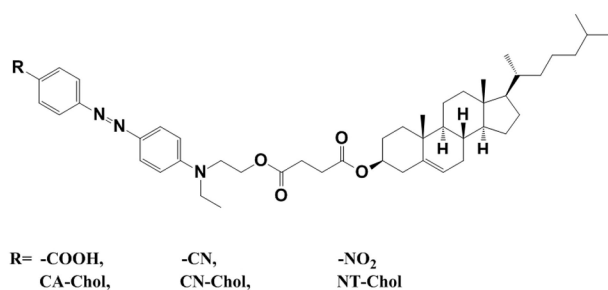


Figure 1. Chemical structure of azo molecular glasses (R-Chol).

Experimental Section

Materials. *N*-Ethyl-*N*-hydroxyethylaniline (97%) was purchased from Tokyo Chemical Industry Co., Ltd. and used as received. 4-Aminobenzonitrile (98%), 4-aminobenzoic acid (98%), and 4-nitroaniline (98%) were purchased from Alfa Aesar and used as received. Tetrahydrofuran (THF) was purified by distillation with sodium and benzophenone. Deionized water (resistivity >18 M Ω cm) was obtained from a Milli-Q water purification

system. Other reagents were commercially available products and used as received without further purification.

Succinic acid cholesteryl ester. Succinic acid cholesteryl ester was prepared according to a literature procedure.^[33] Succinic anhydride (3.3 g, 33 mmol), cholesterol (12.7 g, 33 mmol), and pyridine (0.8 g, 10 mmol) in 300 mL heptane were added to a flask equipped with a magnetic bar. After reaction under reflux for 24 h, the solution was cooled down to room temperature and filtrated. The crude product was purified by recrystallization from acetone. Yield: 70%. ¹H NMR (300 MHz, CDCl₃) δ (ppm): 2.55-2.70 (m, 4H, OOCCH₂CH₂COO), all the other resonance signals on ¹H NMR spectrum represent protons of the cholesteryl group.

2-(*N*-Ethyl-*N*-phenylamino)ethyl 3'-((cholesteryl)oxycarbonyl)propionate. A solution of succinic acid cholesteryl ester (1.5 g, 3 mmol), *N*-ethyl-*N*-hydroxyethylaniline (0.5 g, 3 mmol), *N*, *N*-dicyclohexylcarbodiimide (DCC, 2.4 g, 11 mmol), and 4-dimethylamino pyridine (DMAP, 0.14 g, 1.1 mmol) in 50 mL of dichloromethane was stirred at room temperature for 24 h. Then, *N*, *N*-dicyclohexyl urea was filtered out and the filtrate was washed with water (150 mL), 5% acetic acid solution (150 mL), water again (150 mL), and dried over Na₂SO₄. After evaporating the solvents, the residue was subjected to column chromatography on silica gel with DCM as eluting solvent. Yield: 70%. ¹H NMR (600 MHz, CDCl₃) δ (ppm): 7.23 (t, 2H, ArH), 6.71(m, 3H, ArH), 4.25 (t, 2H, -CH₂-O), 3.55 (t, 2H, -CH₂-N), 3.41 (m, 2H, N-CH₂-CH₃), 1.17 (t, 3H, -CH₃), 2.55-2.70 (m, 4H, OOCCH₂CH₂COO), all the other resonance signals on ¹H NMR spectrum represent protons of the cholesteryl group.

CN-Chol. 4-Aminobenzonitrile (0.6 g, 5 mmol) was dissolved in a mixture of acetic acid (10 mL) and sulfuric acid (1 mL) at 0 °C. NaNO₂ (0.69 g, 10 mmol) dissolved in 1.5 mL water was slowly dripped into the acidified 4-aminobenzonitrile solution. The mixture was stirred in an ice bath for 30 min to obtain the solution of diazonium salt. 2-(*N*-Ethyl-*N*-phenylamino)ethyl 3'-((cholesteryl)oxycarbonyl)propionate (2.5 g, 4 mmol) was dissolved in 50 mL DMF and the solution was cooled down to 0 °C. The diazonium salt solution was added dropwise into the above DMF solution. After reaction for 5 h, the raw product was obtained by pouring the reaction solution into 100 mL deionized water. The precipitate was collected by filtration and washed with excess water until the neutral state was achieved. Purification by column chromatography (silica gel, dichloromethane) yielded red powder in 90% yield. ¹H NMR (600 MHz, CDCl₃) δ (ppm): 7.87 (m, 4H, ArH), 7.73 (d, 2H, ArH), 6.78 (d, 2H, ArH), 4.31 (t, 2H, -OCH₂-), 3.68 (t, 2H, -NCH₂-), 3.52 (q, 2H, -NCH₂CH₃), 2.60 (m, 4H, OOCCH₂CH₂COO), 1.24 (t, 3H, -CH₃), all the other high-field resonance signals in ¹H NMR spectrum represent protons of the cholesteryl group (**Figure S1** in ESI). ¹³C NMR (150 MHz, CDCl₃) δ (ppm): 11.9, 12.4, 18.8, 19.4, 21.1, 22.6, 22.9, 23.9, 24.3, 27.8, 28.1, 28.3, 29.2, 29.4, 31.9, 32.0, 35.9, 36.3, 36.6, 37.0, 38.1, 39.6, 39.8, 42.4, 45.8, 48.8, 50.1, 56.2, 56.8, 61.7, 74.6, 111.5, 112.0, 119.1, 122.8, 126.1, 133.1, 139.6, 143.7, 151.1, 155.6, 171.6, 172.4. IR (KBr, cm⁻¹): 2935, 2902, 2866 (C-H, s), 2224 (C \equiv N, m), 1732 (C=O, s), 1597, 1516 (Benz. ring, s), 1384 (N=N, s), 1254, 1150 (C-O-C, s), 1132 (=N-Ar, s). MS (ESI): calcd. for C₄₈H₆₆O₄N₄ [M + H]⁺: m/z = 763.5157, found: 763.5157. UV-vis: λ_{\max} = 447 nm.

CA-Chol. CA-Chol was similarly prepared as mentioned above for CN-Chol synthesis by using the diazonium salt of 4-aminobenzoic acid. ¹H NMR (600 MHz, CDCl₃) δ (ppm): 8.22 (d, 2H, ArH), 7.90 (m, 4H, ArH), 6.80 (d, 2H, ArH), 4.33 (t,

2H, -OCH₂-), 3.69 (t, 2H, -NCH₂-), 3.53 (q, 2H, -NCH₂CH₃), 2.61 (m, 4H, OOCCH₂CH₂COO), 1.26 (t, 3H, -CH₃), all the other high-field resonance signals in ¹H NMR spectrum represent protons of the cholesteryl group (Figure S1 in ESI). IR (KBr, cm⁻¹): 2945, 2902, 2868 (C-H, s), 1732, 1687 (C=O, s), 1598, 1514 (Benz. ring, s), 1385 (N=N, s), 1244, 1158 (C-O-C, s), 1136 (=N-Ar, s). MS (ESI): calcd. for C₄₈H₆₇O₆N₃ [M + H]⁺: m/z = 782.5108, found: 782.5105. UV-vis: λ_{max} = 432 nm.

NT-Chol. NT-Chol was similarly prepared as mentioned above for CN-Chol synthesis by using the diazonium salt of 4-nitroaniline. ¹H NMR (600 MHz, CDCl₃) δ (ppm): 8.32 (d, 2H, ArH), 7.92 (m, 4H, ArH), 6.79 (d, 2H, ArH), 4.32 (t, 2H, -OCH₂-), 3.69 (t, 2H, -NCH₂-), 3.53 (q, 2H, -NCH₂CH₃), 2.60 (m, 4H, OOCCH₂CH₂COO), 1.25 (t, 3H, -CH₃), all the other high-field resonance signals in ¹H NMR spectrum represent protons of the cholesteryl group (Figure S1 in ESI). IR (KBr, cm⁻¹): 2943, 2903, 2868 (C-H, s), 1733 (C=O, s), 1602, 1518 (Benz. ring, s), 1385 (N=N, s), 1254, 1157 (C-O-C, s), 1135 (=N-Ar, s). MS (ESI): calcd. for C₄₇H₆₅O₆N₄ [M + H]⁺: m/z = 782.4982, found: 782.4980. UV-vis: λ_{max} = 477 nm.

Film preparation. The films with a smooth surface were prepared by spin-coating. The solutions were prepared by dissolving R-Chol in anhydrous THF with a concentration of 5-25% (wt%). The solutions were filtered through 0.45 μm membranes and spin-coated onto the glass slides or CaF₂ (for the case measuring photoinduced dichroism) with a speed about 1500 rpm/min for 30 s. The spin-coated films were dried at room temperature under vacuum for 12 h and then stored in a desiccator for further experiments. The thickness of the films, determined by a scratching method on AFM in contact mode, was controlled to be 0.3-2 μm by adjusting above conditions for different research purposes.

Photoinduced orientation. The optical setup for photoinduced birefringence experiments was similar to those reported previously.^[34] The films were irradiated with a uniform Ar⁺ laser beam (488 nm, 60 mW/cm²). To provide a homogeneous beam profile over the irradiated area of the film, the laser beam was expanded through a spatial filter and collimated. The photoinduced change in the refractive index was probed in a real-time manner by a low-intensity beam from a He-Ne laser (632.8 nm). The probe He-Ne laser beam was transmitted through a pair of crossed polarizers, whose polarization directions were set at ±45° with respect to the polarization of the exciting beam. When the light intensity variation reached the saturated level, the exciting beam was turned off to investigate the relaxation process.

Photoinduced dichroism. Photoinduced dichroism was investigated by polarized FT-IR spectroscopy using the spin-coating films on calcium fluoride disks.^[35] After irradiating with the linearly polarized Ar⁺ laser (488 nm, 60 mW/cm²) for 30 min to induce the orientation, polarized infrared spectra of the samples were obtained at room temperature using the Nicolet 560-IR FTIR spectrophotometer equipped with a wire grid polarizer (KRS-5). The orientation order parameter (S) was calculated by the following equation,

$$S = (A_{\perp} - A_{\parallel}) / (A_{\perp} + 2A_{\parallel}) \quad (1)$$

where A_⊥ and A_∥ are the absorbance perpendicular and parallel to the polarization direction of the laser beam.^[35]

Photoinduced SRG formation. SGRs were inscribed by using the Lloyd mirror set-up according to the literature.^[13,14] A linearly polarized Ar⁺ laser beam (488 nm, 100 mW/cm²) was used as the light source. After the p-polarized laser beam was expanded and collimated, half of the collimated beam was

incident on the films directly and the other half of the beam was reflected onto the films from the mirror. The diffraction efficiency of the first order diffracted beam from the gratings was probed with a low power He-Ne laser beam at 632.8 nm in transmission mode. The surface profiles of the films were probed by AFM on a Nanoscope V instrument in tapping mode.

Two-dimensional quasi-crystal fabrication. The optical setup for two-dimensional quasi-crystal fabrication was similar to those reported previously.^[25] A diode-pumped frequency-doubled solid state laser beam (size~9 mm) with Gaussian profile at 532 nm was split into two equal-intensity beams by using a beam splitter. Two λ/2 wave plates were used to independently rotate the plane of the polarization of the beams. Glan-Thompson prisms were applied to ensure that the electric fields of the two beams were perpendicular to each other (in x and y-axis). Two λ/4 wave plates were put in the optical paths to ensure the interfering beams with opposite circular polarizations (the right-/left-circularly polarized, RCP/LCP). The intensity of each beam was 20-30 mW/cm². The spatial period of the interference pattern (Λ) was controlled by adjusting the intersection angle of the beams (θ), according to the equation λ/(2sin(θ/2)), where λ is the wavelength (532 nm). The irradiation area was about 0.64 cm². CN-Chol films mounted on a rotation stage were exposed to the interference pattern for a fixed period of time. After each exposure, the samples were rotated around the surface normal to achieve the required orientation of the grating vector relative to the previous one. To fabricate a quasi-crystal structure with 2n-fold rotation symmetry, the rotation angle was π/n and n exposure steps were required. Under typical conditions, the time period for each exposure was 5-25 s. The first-order diffraction efficiency was monitored during each writing step. The exact irradiation time for each step was adjusted by controlling the diffraction efficiency to be the same. The two-dimensional quasi-crystal structures on the films were probed by AFM on a Nanoscope V instrument in tapping mode.

Characterization. ¹H NMR and ¹³C NMR spectra were obtained on a JEOL JNM-ECA300 or JEOL JNM-ECA600 NMR spectrometer with tetramethylsilane (TMS) as the internal standard at ambient temperature in CDCl₃. FT-IR spectra were collected on a Nicolet 560-IR spectrometer, the samples were mixed with KBr and then pressed into thin IR-transparent disks. Mass spectra were determined using Thermofisher LTQ system, the sample were dissolved in chloroform. Thermal analyses of the compounds were carried out using TA Instruments DSC Q2000 and TGA Q5000 systems with a heating rate of 10 °C/min in a nitrogen atmosphere. The UV-vis spectra of the samples (THF solutions) were measured by using an Agilent 8453 UV-vis spectrophotometer. The XRD experiments were performed on a RINT2000 vertical goniometer, 185 with a 3 kW ceramic tube as the X-ray source (Cu K_α). Polarizing microscopic observations were conducted on a Nikon LV 1000 POL microscope equipped with a Nikon DS-Fi2 CCD camera, Nikon DS-U3 digital sight, and Linkam LTS420E hot stage. The surface images of SRGs and two-dimensional quasi-crystal structures were monitored using an atomic force microscope (AFM, Nanoscope V) in the tapping mode.

Results and discussion

Synthesis and characterization

The chemical structure of the newly synthesized azo compounds is shown in Figure 1 and the synthetic route is

given in **Scheme S1** (ESI). The molecules contain both an azo chromophore and a cholesteryl group. The molecules differ from each other only in the chromophoric electron-withdrawing groups, which are carboxyl, cyano, and nitro for CA-Chol, CN-Chol, and NT-Chol, respectively. All the target molecules were obtained from the same precursor, 2-(*N*-ethyl-*N*-phenylamino)ethyl 3'-((cholesteryl)oxycarbonyl)propionate. It was then reacted with the diazonium salts of the corresponding amino compounds through the azo-coupling reaction. This reaction route can introduce azo chromophores with different electron-withdrawing groups at the final stage of the preparation under mild conditions, which is suitable to prepare a series of similar azo molecules bearing different electron-withdrawing groups. The ^1H NMR spectra of the target molecules CA-Chol, CN-Chol and NT-Chol are given in **Figure S1** (ESI) with the resonance signal assignments. The multiple resonance signals at the high magnetic field are from the protons of the cholesteryl unit. The other resonances can be well assigned to the chemical structure as given in **Figure 1**. The structures of the newly synthesized molecules are also verified by FT-IR, MS and UV-Vis.

The thermal transitions and phase behaviour of R-Chol (R=CA, CN or NT) were investigated by DSC, XRD and POM. **Figure 2** shows the DSC curves of R-Chol on the second-heating and the second-cooling scans. R-Chol (R=CA, CN or NT) shows both the properties of glassy materials and liquid

crystal (LC) depending on the temperature. The glass transition can be seen when the temperature increases. After glass transition, the materials enter the liquid crystalline phase as indicated by POM and XRD. The phase transition occurs in the high temperature range of the DSC curves is the liquid crystal/isotropic (LC/I) transition. The T_g and $T_{LC/I}$ obtained from the DSC are summarized in **Table 1**. CA-Chol containing the 4-carboxylazobenzene moiety shows the highest T_g and $T_{LC/I}$ values among the compounds. It can be attributed to the hydrogen bonding between the COOH groups as confirmed by IR from the wavenumber shift of the peak at 1687 cm^{-1} (**Figure S2** in ESI).³⁶ The liquid crystal textures of R-Chol (R = CA, CN or NT) observed with POM are given in **Figure S3** (ESI). The XRD measurements indicate that the R-Chol form the smectic phase in the LC state (**Figure S4** in ESI).

Table 1. The glass transition temperature (T_g), liquid crystal/isotropic transition temperature (T_{LC-I}) and λ_{max} of R-Chol.

Sample	T_g ($^{\circ}\text{C}$) ^a	$T_{LC1/LC2}$ ($^{\circ}\text{C}$) ^a	$T_{LC2/I}$ ($^{\circ}\text{C}$) ^a	λ_{max} (nm) ^b
CA-Chol	54	-	171	433
CN-Chol	31	63	76	448
NT-Chol	30	-	119	477

^a From the heating scans. ^b THF solutions.

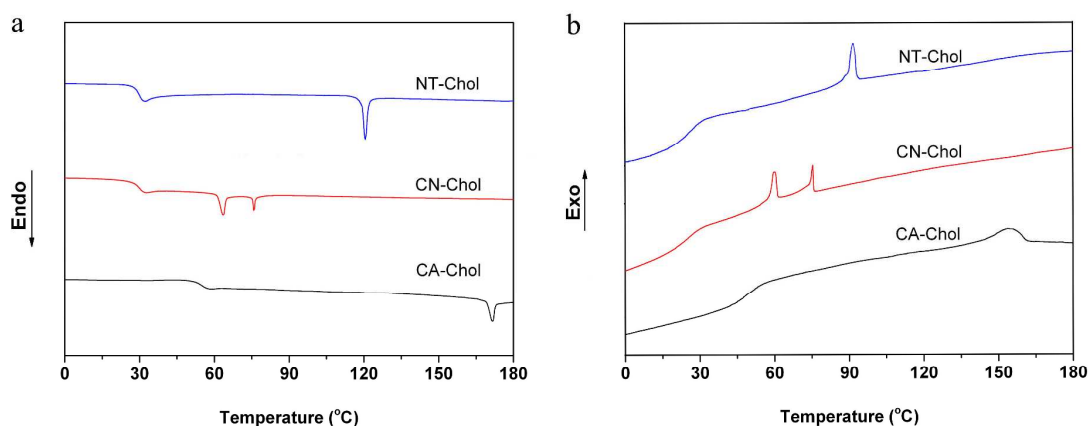


Figure 2. DSC curves of R-Chol series compounds for the second heating and second cooling scans.

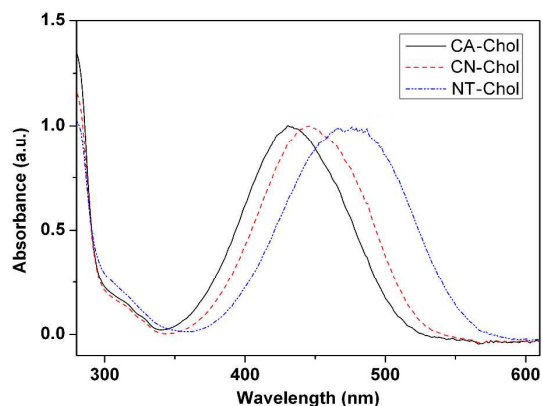


Figure 3. UV-vis spectra of the azo compounds in THF.

The UV-vis spectra of the azo compounds in THF solutions are shown in **Figure 3**, which possess typical spectral features of pseudo-stilbene-type azo compounds. The absorption bands corresponding to the $\pi \rightarrow \pi^*$ transition appear at the longest wavelength and the azo compounds show strong absorption in the visible region. The positions of the absorption bands are strongly affected by the electron-withdrawing groups on the azobenzene moieties. The λ_{max} s of CA-Chol, CN-Chol and NT-Chol are 433, 448, and 477 nm (Table 1). This tendency reflects their inductive and conjugative strength for both the ground and the excited states.

Photoinduced birefringence and dichroism

The solid thin films with smooth surface were prepared by spin-coating for all the following investigations. As THF was quickly evaporated during the spin-coating process, only NT-Chol film shows weak birefringence and polydomain texture as

indicated by the POM observation (**Figure S5** in ESI). For the other two compounds, no birefringence could be observed. The DSC measurements were performed by using solid samples collected from the spin-coated R-Chol films and the DSC curves are given in **Figure S6** (ESI). Only NT-Chol shows the endothermic transition corresponding to T_{LCI} transition. These results indicate that the CA-Chol and CN-Chol exist in the amorphous state for the spin-coated films under the processing conditions. Only NT-Chol shows liquid crystallinity with the local low orientational order.

Photoinduced birefringence of CA-Chol, CN-Chol and NT-Chol were investigated in a real-time manner by irradiating the solid thin films of CA-Chol, CN-Chol and NT-Chol with a linearly polarized laser beam (60 mW/cm²) at 488 nm as described in the experimental section. The photoinduced birefringence was calculated from the detected transmittance of the probing laser by the equation,^[37]

$$I = I_0 \sin^2(\pi \Delta n d / \lambda) \quad (2)$$

where I is the intensity of the light transmitted through the crossed polarizer, I_0 is the intensity of the probe beam transmitted through the first polarizer, λ is the wavelength of the probe wave (633 nm), d is the film thickness, and Δn is the birefringence.

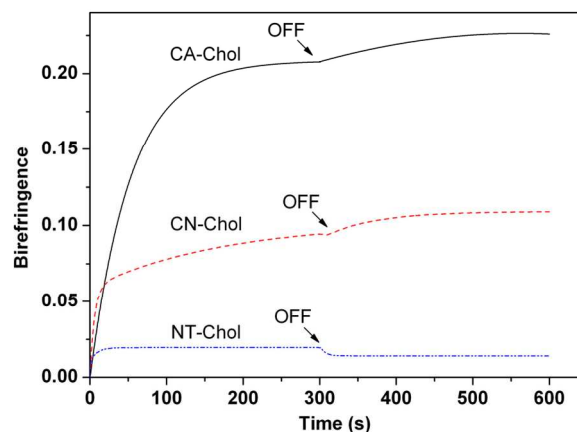


Figure 4. The variations of the photoinduced birefringence of R-Chol thin films with the irradiation time and relaxation time.

Figure 4 shows variations of the photoinduced birefringence of the R-Chol thin films with the irradiation time. Before the excitation laser was switched on, no transmittance of the probing laser beam can be detected by the photodiode, because the sample placed between the crossed polarizers is isotropic. It indicates that although mesogenic groups in NT-Chol possess local orientational order, the film is polydomain and isotropic in macroscopic level in the film plane. As homeotropical alignment is typical in smectic LC, the predominant orientational direction of the mesogenic groups could be perpendicular to the substrate surface. When the writing laser beam is switched on, the birefringence increases rapidly at the initial stage and is then gradually saturated after the rapid increase. The saturated birefringence of CA-Chol is the highest in the series, which can reach 0.21. This value is much higher compared with those for most azo polymers.^[2,4,5] The saturated birefringence of NT-Chol is much smaller compared with the values of its counterparts, which is only 0.02. The photoinduced birefringence behaviour of the azo molecular glasses is closely correlated with the effect of the electron-withdrawing groups on

the azobenzene moieties.^[29,31] For both amorphous molecular materials and azo polymers, the similar tendency has been observed for these electron-withdrawing groups to affect the birefringence growth and saturated values.^[31,32,36,38] It reflects the influence of the electron-withdrawing groups on the photoinduced orientation ability at the molecular level. On the other hand, the extremely low degree of the photoinduced birefringence of NT-Chol could also be related with the liquid crystallinity of the film. If the alignment of azo chromophores is perpendicular to film surface (homeotropical orientation), the light absorption should be weak as the transition moment is perpendicular to the vibration direction of the electric field of the light wave. Therefore, it will result in a low isomerization degree of the azo chromophores. Moreover, the photoinduced isomerization of the azobenzene moieties in NT-Chol film could be less efficient due to the tight packing of the chromophores to form the LC phase.

For azo polymers and related materials, the photoinduced Δn usually decreases in some degree when the writing laser beam is switched off.^[2,4,5,33,36,38-40] In contrast to the typical decay relaxation, no birefringence decrease is observed for CA-Chol and CN-Chol after switching off the irradiating light (**Figure 4**). Even a slight increase in the birefringence can be observed after switching off the irradiating light, which has also been observed for other amorphous molecular materials with a linear molecular structure.^[31,32]

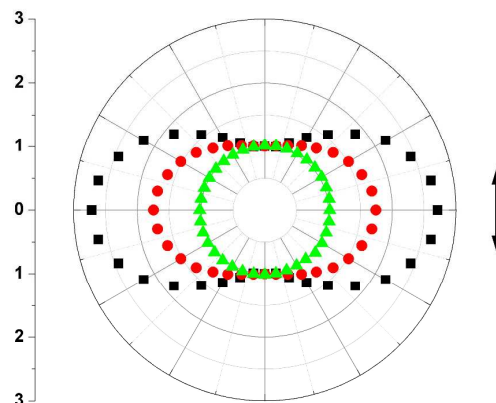


Figure 5. The polar plots of the relative infrared absorbance of stretching vibration bands of the $\nu(\text{C}=\text{C})$ (aromatic, 1599 cm⁻¹ for CA-Chol (■), 1597 cm⁻¹ for CN-Chol (●), and 1601 cm⁻¹ for NT-Chol (▲)) of the R-Chol films.

The photoinduced dichroisms of the R-Chol films were characterized using polarized FT-IR spectroscopy. **Figure 5** gives the polar plots of the relative infrared absorbance of the stretching vibration bands of $\nu(\text{C}=\text{C})$ (aromatic) for the R-Chol films, which are 1599 cm⁻¹ for CA-Chol, 1597 cm⁻¹ for CN-Chol, and 1601 cm⁻¹ for NT-Chol. In this experiment, the R-Chol films were irradiated with a linearly polarized Ar⁺ laser beam (488 nm, 60 mW/cm²) till the saturation and then polarized FT-IR spectra were obtained at different angles relative to the polarization plane. The orientation order parameter (S) was calculated by Equation 1. The orientation order parameters derived from the angular-dependent IR absorption are 0.461, 0.199 and 0.001 for CA-Chol, CN-Chol and NT-Chol, respectively. The orientation order parameters show the same order as indicated by the birefringence measurements. The orientation order parameter of CA-Chol is much higher than the ordinary values of azo polymers.^[2,4,5,33,38]

The low orientational order parameters of NT-Chol could be attributed to the same reasons discussed above.

Photoinduced SRGs and surface quasi-crystal structures

The properties of the amorphous molecular materials to form surface relief gratings (SRGs) and other surface relief patterns were investigated. SRGs were inscribed by exposing the spin-coated solid films of R-Chol to the interference patterns formed by the two p -polarized laser beams (polarization in the plane of incidence), which is typically used in previous study.^[14] The Ar^+ laser beam with the wavelength of 488 nm (100 mW/cm^2) was used as the writing light and a low intensity He-Ne laser beam (632.8 nm) was used as the probe beam. The profiles and trough depths of the gratings were detected by AFM.

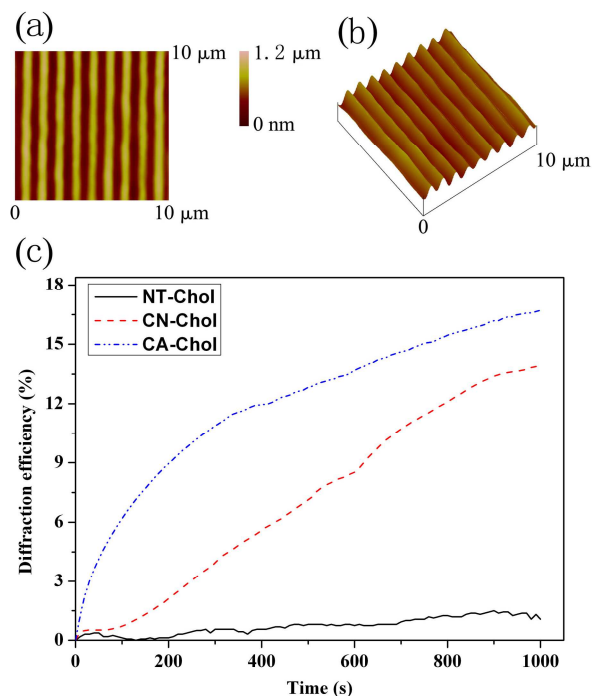


Figure 6. a) and b), typical AFM images of the sinusoidal surface relief structures on the films of CA-Chol after irradiation for 30 min; c), the first order diffraction efficiency as a function of the irradiation time in the process of SRG formation on the films of R-Chol.

Figure 6a and **6b** show typical AFM images of the sinusoidal surface relief structures. The SRGs with regular spaces are formed on the films of CA-Chol after irradiated with the interfering Ar^+ laser beams (488 nm) for 30 min. The sinusoidal surface patterns with a period about $1 \mu\text{m}$, which depends on the wavelength and the incident angle of the writing beams,^[13,14] can be seen from the images. The average amplitude of the SRG inscribed on the surface of the CA-Chol film can reach $1 \mu\text{m}$ for the film with a thickness about $2 \mu\text{m}$. The SRG formation was also monitored by measuring the diffraction efficiencies of the probe beam in a real-time manner. **Figure 6c** presents the first order diffraction efficiency as a function of the irradiation time in the process of SRG formation on the films of CA-Chol, CN-Chol and NT-Chol. The diffraction efficiencies for the CA-Chol, CN-Chol and NT-Chol gratings are 0.17, 0.14 and 0.01 after irradiation for 1000 s, respectively. The result shows that CA-Chol has the highest

growth rate for SRG formation in the series. This tendency is the same as the photoinduced birefringence growth rate (**Figure 4**).

Two-dimension (2D) quasi-crystal surface patterns on R-Chol films were fabricated by dual-beam multiple exposure technique.^[25] In each step, the spin-coated films of R-Chol were exposed to the interference patterns formed by beams with opposite circular polarizations (LCP/RCP). A diode-pumped frequency-doubled solid state laser beam (size $\sim 9 \text{ mm}$) with Gaussian profile at 532 nm (30 mW/cm^2) was used as the excitation light. After each exposure, the films were rotated around the surface normal to achieve the required orientation of the grating vector relative to the previous one. The profiles and trough depths of the surface quasi-crystal structures were detected by AFM.

Figure 7a and **7b** give the AFM images of the quasi-crystal patterns with 12-fold symmetry on the CN-Chol film. The quasi-crystal structures on the surfaces were fabricated through 6 exposure steps by using the interference pattern with the period of $6.2 \mu\text{m}$. **Figure 7c** and **7d** give the typical optical micrograph of the quasi-crystal structures in the transmittance and refractive modes respectively, which show the quasi-crystal patterns in a large scale. **Figure 7e** gives the diffraction pattern of a He-Ne laser beam with normal incidence to the sample. The quasi-crystal structures with other folds of the symmetry are shown in **Figure S7** (ESI). The quasi-crystal structures with different rotation symmetry can be prepared on CN-Chol films through this procedure. Although the CA-Chol film has the higher efficiency to form SRG than that of CN-Chol, the quasi-crystal structures with such high quality cannot be inscribed on CA-Chol film under the same condition. It indicates that although both SRG and quasi-crystal surface pattern are formed by the photoinduced mass transport, the fabrication of the quasi-crystal surface patterns shows stricter requirements for other material properties, such as the mechanical response parameters to the deformation.

Holographic recording

The performance of the amorphous molecular materials as holographic recording medium was tested by using typical two-beam interference technique. The scheme of the holographic recording is given in **Figure S8** (ESI). A diode-pumped frequency-doubled solid state laser (532 nm) was used as the light source. A piece of the spin-coated film of CA-Chol was used as the recording medium. The film with the smooth surface was exposed to the interference pattern formed by the object wave and the coherent reference wave. In the process, the laser beam with Gaussian profile was split into two equal-intensity beams by using a beam splitter. Both beams were linearly polarized to possess the s -polarization (polarization perpendicular to the plane of incidence). One beam whose size was controlled by a lens irradiated onto the CA-Chol film directly. The image of the panda was recorded by the other beam after expanded by two lenses. The object wave then irradiated onto the same area of the film after collimated by the third lens. The whole holographic recording process was completed in 5–20 s. After recording the image, a He-Ne laser (633 nm) was used as the reference wave to read out the holographic pattern recorded in the film.

Figure 8 gives the original picture and the image read out by the reference wave. It can be seen that the panda image can be vividly recorded in the hologram. The image is recorded by the photoinduced volume birefringence to achieve the polarization holographic recording. As surface modulation can

also be induced on the film, the image becomes blurred after irradiation for a longer time. As both processes possess very different time scales, where the polarization grating formation is completed in a much shorter time period, the polarization holographic recording can be achieved by controlling the writing time. This problem can also be solved by sandwiching the thin film in two-pieces of the glass slides.^[41]

Conclusions

A series of liquid-crystalline compounds containing strong *push-pull* azo chromophores and cholesteryl unit (R-Chol, R: CA, CN and NT) was developed as novel molecular glasses. The azo compounds exist as glassy solid at room temperature, whose phases of the condensed states depend on molecular structures and processing conditions. In the thermodynamic equilibrium state, the molecular materials show smectic liquid crystallinity above their glass transition temperature. On the other hand, by using a volatile solvent THF, the spin-coated

films of CA-Chol and CN-Chol exist in the amorphous state and only NT-Chol film shows weak birefringence and polydomain texture. At the room temperature, the amorphous molecular glass films show a very sensitive response to the light irradiation as exhibited by the photoinduced birefringence, dichroism and SRG formation. The birefringence and the orientation order parameters of the CN-Chol and CA-Chol films are much higher than those of typical azo polymers and NT-Chol. When the irradiating light is switched off, no orientation relaxation occurs and the birefringence even increases slightly. The SRGs can be formed on CN-Chol and CA-Chol films with the high efficiency. Two-dimensional (2D) quasi-crystal structures with 10- and 12- rotation symmetries are successfully fabricated on the CN-Chol films by using the dual-beam multiple exposure technique. By using one of the molecular glasses, CA-Chol, the application of the materials as holographic medium is demonstrated.

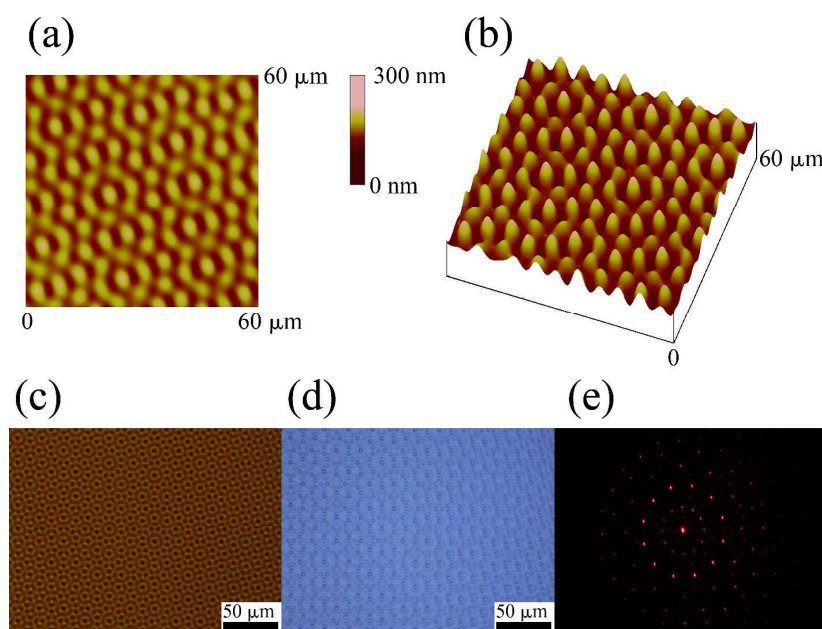


Figure 7. The 12-fold quasi-crystal produced with the $\Lambda = 6.2 \mu\text{m}$ interference pattern on the film of CN-Chol: (a) AFM 2D-view image, (b) AFM 3D-view image, (c) optical micrograph in transmittance mode, (d) optical micrograph in refractive mode, (e) photograph of the He-Ne laser diffraction pattern.



Figure 8. The original panda image and the image read out from hologram by the reference wave.

ARTICLE

Acknowledgements

The financial support from NSFC under project 51233002 is gratefully acknowledged.

Notes and references

^a Department of Chemical Engineering, Laboratory of Advanced Materials (MOE), Tsinghua University, Beijing 100084, P. R. China.

Tel: 86-10-62784561, Fax: 86-10-62770304, email: wxg-dce@mail.tsinghua.edu.cn.

^b Current Address: Research Branch of Advanced Functional Materials, School of Microelectronics and Solid-State Electronics, High Temperature Resistant Polymer and Composites Key Laboratory of Sichuan Province, University of Electronic Science and Technology of China, Chengdu, 610054, P. R. China.

^c Department of Physics, School of Science, Beijing University of Aeronautic and Astronautic, Beijing 100083, P. R. China

†

Electronic Supplementary Information (ESI) available: [More results of the syntheses and characterization can be seen there]. See DOI: 10.1039/b000000x/

- G. S. Kumar, D. C. Neckers, *Chem. Rev.*, 1989, **89**, 1915-1925.
- S. Xie, A. Natansohn, P. Rochon, *Chem. Mater.* 1993, **5**, 403-411.
- N. K. Viswanathan, D. Y. Kim, S. P. Bian, J. Williams, W. Liu, L. Li, L. Samuelson, J. Kumar, S. K. Tripathy, *J. Mater. Chem.* 1999, **9**, 1941-1955.
- J. A. Delaire, K. Nakatani, *Chem. Rev.* 2000, **100**, 1817-1845.
- A. Natansohn, P. Rochon, *Chem. Rev.*, 2002, **102**, 4139-4175.
- T. Ikeda, J. Mamiya, Y. L. Yu, *Angew. Chem., Int. Ed.*, 2007, **46**, 506-528.
- Y. Zhao, *Macromolecules* 2012, **45**, 3647-3657.
- H. F. Yu, T. Ikeda, *Adv. Mater.*, 2011, **23**, 2149-2180.
- S. Lee, H. S. Kang, J. K. Park, *Adv. Mater.*, 2012, **24**, 2069-2103.
- D. R. Wang, X. G. Wang, *Prog. Polym. Sci.*, 2013, **38**, 271-301.
- H. Rau, *Photoisomerization of azobenzenes. In: Rabek JF, editor. Photochemistry and photophysics.* Boca Raton (FL): CRC Press, 1990.
- T. Todorov, L. Nikolova, N. Tomova, *Appl. Opt.*, 1984, **23**, 4309-4312.
- P. Rochon, E. Batalla, A. Natansohn, *Appl. Phys. Lett.*, 1995, **66**, 136-138.
- D. Y. Kim, S. K. Tripathy, L. Li, J. Kumar, *Appl. Phys. Lett.*, 1995, **66**, 1166-1168.
- T. Ikeda, S. Horiuchi, D. B. Karanjit, S. Kurihara, S. Tazuke, *Macromolecules*, 1990, **23**, 42-48.
- C. Hubert, C. Fiorini-Debuisschert, I. Maurin, J. M. Nunzi, P. Raimond, *Adv. Mater.*, 2002, **14**, 729-732.
- H. Finkelmann, E. Nishikawa, G. G. Pereira, M. Warner, *Phys. Rev. Lett.* 2001, **87**, 015501 (4 pages).
- M. H. Li, P. Keller, B. Li, X. G. Wang, M. Brunet, *Adv. Mater.* 2003, **15**, 569-572.
- Y. L. Yu, M. Nakano, T. Ikeda, *Nature* 2003, **425**, 145-145.
- Y. B. Li, Y. N. He, X. L. Tong, X. G. Wang, *J. Am. Chem. Soc.*, 2005, **127**, 2402-2403.
- Y. Shiota, *J. Mater. Chem.*, 2005, **15**, 75-93.
- H. Nakano, T. Takahashi, T. Kadota, Y. Shiota, *Adv. Mater.*, 2002, **14**, 1157-1160.
- E. Ishow, C. Bellaïche, L. Bouteiller, K. Nakatani, J. A. Delaire, *J. Am. Chem. Soc.*, 2003, **125**, 15744-15745.
- M. J. Kim, E. M. Seo, D. J. Vak, D. Y. Kim, *Chem. Mater.*, 2003, **15**, 4021-4027.
- M. C. Guo, Z. D. Xu and X. G. Wang, *Langmuir*, 2008, **24**, 2740-2745.
- L. M. Goldenberg, L. Kulikovskiy, O. Kulikovska, J. Tomczyk, J. Stumpe, *Langmuir*, 2010, **26**, 2214-2217.
- Z. T. Nagy, B. Heinrich, D. Guillon, J. Tomczyk, J. Stumpe, B. Donnio, *J. Mater. Chem.*, 2012, **22**, 18614-18622.
- J. Tomczyk, A. Sobolewska, Z. T. Nagy, D. Guillon, B. Donnio, J. Stumpe, *J. Mater. Chem. C*, 2013, **1**, 924-932.
- J. J. Yin, G. Ye, X. G. Wang, *J. Mater. Chem. C*, 2013, **1**, 3794-3801.
- Z. Xie, H. F. He, Y. H. Deng, X. G. Wang, C. Y. Liu, *J. Mater. Chem. C*, 2013, **1**, 1791-1797.
- G. Ye, D. R. Wang, Y. N. He, X. G. Wang, *J. Mater. Chem.*, 2010, **20**, 10680-10687.
- Y. W. Wang, G. Ye, X. G. Wang, *J. Mater. Chem.*, 2012, **22**, 7614-7621.
- Y. Zhu, Y. Q. Zhou, Z. Chen, R. Lin, X. G. Wang, *Polymer*, 2012, **53**, 3566-3576.
- A. Natansohn, P. Rochon, J. Gosselin, S. Xie, *Macromolecules* 1992, **25**, 2268-2273.
- T. Buffeteau, M. Pézolet, *Macromolecules* 1998, **31**, 2631-2635.
- Y. W. Wang, Y. N. He, X. G. Wang, *Polym. Bull.*, 2012, **68**, 1731-1746.
- A. Saishoji, D. Sato, A. Shishido, T. Ikeda, *Langmuir*, 2007, **23**, 320-326.
- X. L. Wang, J. J. Yin and X. G. Wang, *Polymer*, 2011, **52**, 3344-3356.
- Y. Zhu, X. G. Wang, *Dyes and Pigments*, 2013, **97**, 222-229.
- Y. Zhu, Y. Q. Zhou and X. G. Wang, *Dyes and Pigments*, 2013, **99**, 209-219.
- M. C. Guo, Z. D. Xu, X. G. Wang, *Optical Materials*, 2008, **31**, 412-417.

Graphical Abstract

Liquid-Crystalline Compounds Containing Both Strong *Push-Pull*
Azo Chromophore and Cholesteryl Unit as Photoresponsive
Molecular Glass MaterialsRenbo Wei,^a Zeda Xu^b, Xiyang Liu,^a Yaning He,^a and Xiaogong Wang^{a*}^a Department of Chemical Engineering, Laboratory of Advanced Materials
(MOE), Tsinghua University, Beijing 100084, P. R. China.^b Department of Physics, School of Science, Beijing University of Aeronautic and
Astronautic, Beijing 100083, P. R. China